Hydrocarbon - Air - Nitrous Oxide Detonations

M. Kaneshige
Mechanical Engineering

R. Akbar, J.E. Shepherd
Graduate Aeronautical Laboratories

California Institute of Technology

April 14-15, 1997

Western States Section
Combustion Institute
Spring Meeting

Abstract

We are investigating the properties of explosive gas mixtures containing H_2, CH_4, N_2O, O_2, and N_2 that may be present within the vapor space of waste storage tanks. Several series of experiments have been performed to measure the detonation cell sizes of these mixtures. Cell size data can be correlated to detonation initiation and propagation limits, and can also be used to validate chemical kinetics models. The facility used is the GALCIT Detonation Tube, which has a 280 mm inside diameter and is 7.3 m long. Initiation is by an acetylene-oxygen driver and an exploding electric wire. Tube performance is monitored by pressure transducers and cell sizes are measured from sooted foils.

Three series of tests with mixtures of $H_2 + N_2O + \alpha\ O_2 + \beta\ N_2$, $CH_4 + 2O_2 + \beta\ N_2$, and $CH_4 + 4N_2O + \beta\ N_2$ have been performed. Cell size has been measured as a function of dilution and initial pressure, up to the limits of the facility. Mixtures were limited in detonation pressure by the tube structural strength and by the minimum tube diameter for detonation propagation. As the dilution was increased in each series, the initial pressure was decreased to remain within the structural limitation. While cell size is notoriously difficult to measure because of spatial and temporal nonuniformities, it is consistently found to increase with increasing dilution and decrease with increasing initial pressure. Cell width increases rapidly with increasing dilution as the propagation limits are approached.

We have carried out detailed kinetic modeling of the ZND structure of detonations in order to correlate cell width to reaction zone length. The chemical reaction mechanisms and rates have been validated by comparing computations of induction times to shock tube measurements.

Introduction

Detonation hazards are typically characterized by several detonability parameters (critical energy, critical tube diameter, minimum tube diameter) that can each be related to the detonation cell width, which provides a convenient measurable length scale. The novel mixtures encountered in some waste tanks provide a challenge because cell width data are scarce and the mixtures are sensitive to small changes in some variables (e.g. N_2O and O_2 concentrations). One approach to determining the detonability of the mixtures of interest is to measure cell widths under a range of possible conditions. Another, complementary approach, is to compute reaction zone thicknesses behind idealized detonation waves, derive a correlation between measured cell widths and these computed reaction zone thicknesses, and use the correlation to predict cell widths at untested conditions. Reaction zone calculations rely on detailed reaction rate mechanisms, so some effort is required to ensure that the calculations are meaningful. However, the empirical correlation to cell width masks some uncertainty in the calculations. Following this combined approach, cell width data of direct usefulness to hazard analysis are generated and a rational means of interpolating and extrapolating these data is developed. Current efforts involve extending the experimental database and improving the correlations.

Apparatus and Procedure

The experimental facility used was the GALCIT Detonation Tube. It is 7.3 m long with 280 mm inner diameter and is constructed of 3 cast stainless steel (304) segments (Fig. 1). The assembly is mounted on linear bearings to allow for maintenance and recoil. The gas supply system can deliver H_2, N_2O, N_2, NH_3, CH_4, O_2, or other gases as required, from an external cylinder farm. The tube is typically evacuated to 50 millitorr before filling. Mixtures are created by the method of partial pressures to obtain the desired concentrations. Test mixtures are circulated through the tube and a parallel line by a bellows pump before firing. A number of instrumentation ports allow access along the tube, and pressure traces are typically taken at three points.

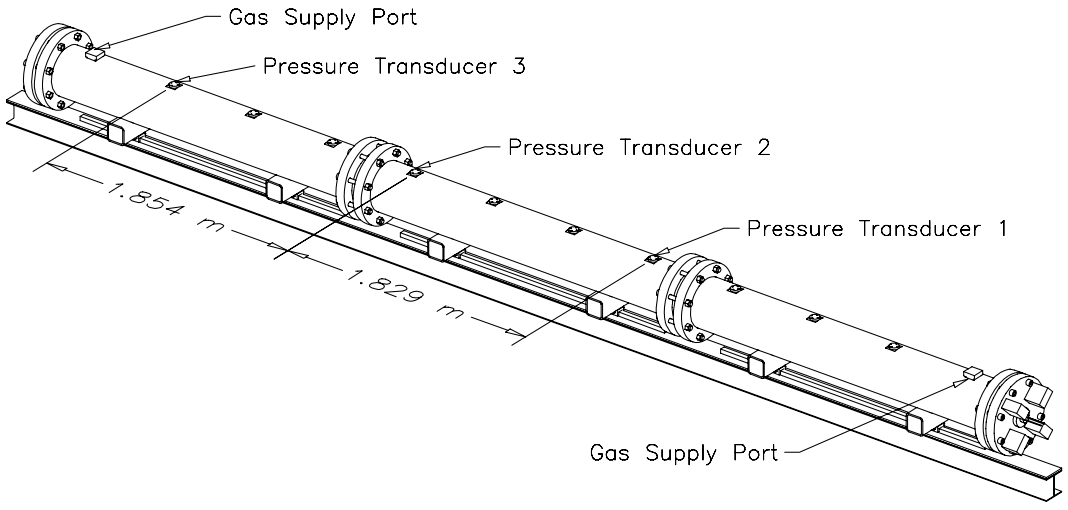

Figure 1: GALCIT Detonation Tube

Detonation initiation is performed by an oxy-acetylene driver to reliably obtain detonations in all mixtures capable of propagating in the tube. A programmable control system injects a mixture of acetylene and oxygen for a given time period and then triggers an exploding wire after a given delay. The exploding wire is driven by a 2 μF capacitor bank charged to about 10 kV and switched through a spark gap. The acetylene - oxygen ratio is controlled by individual pressure regulators. A study has been conducted to characterize the driver, and it has been found to be capable of controllably delivering an equivalent of 10-120 kJ initiation energy. This control allows very nearly Chapman-Jouguet detonations to be initiated in mixtures with a wide range

of sensitivities.

Cell widths are measured by the soot foil technique. The foils are 2-ft x 3-ft x 0.020-in thick aluminum and are rolled into cylinders to conform to the detonation tube inner diameter. Each foil is sooted over a fuel-rich kerosene flame. The cell widths are measured on flattened foils, as the transverse distance between triple point tracks. Since this distance can vary significantly over a foil, minimum and maximum values are reported. Note that for small cells (relative to the tube diameter), this is an unique measure of the cell width, but for cell widths on the order of the tube diameter, this measure may not be comparable to measurements in other facilities or by other techniques. In this case, the effect of the tube geometry on the cells should be considered when interpreting the data.

Table 1: Experimental Tests

Test	Mixture	Press. kPa	Go	D_{CJ} m/s	D_{1-2} m/s	D_{2-3} m/s	λ_{min} mm	λ_{max} mm
17	H_2+N_2O+2air	100.0	Yes	1937	1928	1923	4	5
18	H_2+N_2O+3air	100.0	Yes	1806	1794	1787		
19	H_2+N_2O+3air	100.0	Yes	1806	1792	1787	4	6
20	H_2+N_2O+4.7air	100.0	Yes	1637	1618	1610	60	80
22	H_2+N_2O+8air	100.0	No					
23	H_2+N_2O+5.7air	100.0	Yes	1554	1546	1521	110	150
24	H_2+N_2O+6.3air	100.0	DDT	1521	1807	1440	80	100
25	H_2+N_2O+2air	100.0	Yes					
26	H_2+N_2O+2N_2	100.0	Yes	1962	1947	1947	7	10
27	H_2+N_2O+3N_2	100.0	Yes	1839	1812	1814	15	30
29	H_2+N_2O+3.6N_2	100.0	No					
30	H_2+N_2O+3.3N_2	100.0	Yes	1810	1780	1779		
31	H_2+N_2O+3.3N_2	100.0	DDT	1810				
32	H_2+N_2O+3.3N_2	100.0	Yes	1810	1775	1778		
33	H_2+N_2O+3.3N_2	100.0	Yes	1810	1780	1777	15	25
34	H_2+N_2O+3.9N_2	100.0	Yes	1746	1710	1713		
35	H_2+N_2O+4.3N_2	100.0	Yes	1711	1668	1671		
36	H_2+N_2O+4.7N_2	100.0	Yes	1674	1644	1621		
37	H_2+N_2O+5.1N_2	100.0	No					
39	H_2+N_2O+5.1N_2	100.0	Yes	1633	1605	1598		
40	H_2+N_2O+4.7N_2	100.0	No					
46	H_2+N_2O+4.7N_2	100.0	Yes	1674	1649	1637	150	300
51	CH_4+2O_2	72.1	Yes	2378	2815	2761	4.5	9
52	CH_4+2O_2[1]	72.1	Yes	2378	2440	2434	2.5	5
53	CH_4+2O_2	72.2	Yes	2378	2528	2387	4	10
54	CH_4+2O_2+2N_2	89.2	Yes	2109	2125	2117	10.5	23.5
55	CH_4+2O_2+4N_2	102.2	Yes	1969	1978	1979	30	55.5
56	CH_4+2O_2+5N_2	102.2	Yes	1915	1918	1909	57.5	84.5
57	CH_4+2O_2+6N_2	72.2	Yes	1860	1867	1856	161	295
76	CH_4+4N_2O	57.2	Yes	2179	2186	2179	3.5	8
77	CH_4+4N_2O+N_2	62.2	Yes	2114	2121	2119	7.5	14.5
78	CH_4+4N_2O+2N_2	72.2	Yes	2063	2070	2065	10	19
79	CH_4+4N_2O+3N_2	77.2	Yes	2016	2020	2018	13.5	20
80	CH_4+4N_2O+4N_2	82.2	Yes	1975	1978	1977	16.5	49
81	CH_4+4N_2O+5N_2	87.2	Yes	1938	1941	1931	24	42.5
85	CH_4+4N_2O+6N_2	92.2	Yes	1903	1906	1901	24	60
86	CH_4+4N_2O+7N_2	97.2	Yes	1871	1873	1863	39.5	80
87	CH_4+4N_2O+8N_2	102.2	Yes	1899	1841	1828	54	68
88	CH_4+4N_2O+9N_2	102.3	Yes	1812	1805	1784	61	96
90	CH_4+4N_2O+9N_2	102.2	No	1812	528	504	-	-
91	CH_4+4N_2O+8.5N_2	102.2	Yes	1826	1828	1807	71	107

[1]Contaminated with about 2% C_2H_2

The condition of primary interest is 1 atm and about 298 K, but structural limitations prevent the use of low dilution at 1 atm for some mixtures. In each test series, as the dilution was increased, the initial pressure was increased such that predicted detonation pressures were just below the tube design limit, up to 1 atm initial pressure. Dilution was further increased to the propagation limit of the tube. The largest cell sizes possible are about 50% to 100% of the tube diameter.

Experimental Results

Four sets of experiments have been performed, with mixtures consisting of $H_2 + N_2O + \beta\ N_2$, $H_2 + N_2O + \beta$ air, $CH_4 + 2O_2 + \beta\ N_2$, and $CH_4 + 4N_2O + \beta\ N_2$. Soot foil and pressure history records were made for a range of dilution ratio and initial pressure, yielding cell width and detonation velocity data.

The cell measurements and detonation velocities for a number of tests with these mixtures are shown in Table 1. Apparent detonation velocities between pressure transducers 1 and 2 and between 2 and 3 are reported under D_{1-2} and D_{2-3}. For comparison, the CJ velocities (computed by Stanjan equilibrium code) are listed and are remarkably close to the measured velocities. Reported initial pressure includes the pressure added by injection of the driver gas. The H_2-N_2O data show that air dilution results in smaller cell widths than N_2 dilution. This is a systematic effect resulting from the preferential oxidation of H_2 by O_2 over N_2O. Cell widths versus computed reaction zone thickness are also shown in Figs. 6, 7, and 8 (discussed later).

Chemical Kinetics Modeling

Cell width for complex chemical systems can not currently be computed by direct numerical simulation. One goal of our work is to develop the capability to predict cell widths through chemical kinetics calculations and a correlation between the kinetics results (typically reaction zone thickness) and cell width. A prerequisite is the ability to accurately model the chemical kinetics.

The reactions of interest in this study involve the oxidation of H_2 and CH_4 by N_2O and air. The chemistry of the individual fuel-oxidizer combinations have been studied in some detail, but few studies are available with combinations of these fuels and oxidizers. The number of relevant studies is further reduced by the limited conditions considered in each. Reaction models have been developed to treat the chemistry of the individual fuel-oxidizer systems. Mechanisms can be built and expanded from the simple and better understood reactions to the more complicated systems of interest. One goal of our theoretical work is to find or create a mechanism capable of accurately modeling mixtures that contain H_2, N_2O, NH_3, CH_4, and air. The intermediate goal is to accurately model simpler mixtures. H_2-N_2O-diluent, CH_4-O_2-diluent, and CH_4-N_2O-diluent mixtures have been tested experimentally to validate these theoretical efforts.

All chemical kinetics simulation has been done within the framework of the Sandia gas phase chemical kinetics subroutine package (Kee et al. (1989)). This package consists of a set of Fortran library functions that can be called from within a simulation program.

Reaction Mechanism Validation

A study to determine the limits of validity of several published mechanisms under detonation-like conditions has been conducted. Computational results using the different mechanisms were compared with published data from shock tube experiments. The reflected shock experiments were modeled as constant volume processes. Induction time was used as the basis of comparison because it is sensitive to accurate modeling and concisely characterizes the explosion process. Since relative measurements can be used to determine induction time, detection or measurement do not need to be quantitative and data analysis is simplified. Induction time is also closely related to reaction zone thickness in detonations.

Numerical Technique

The model used to simulate the shock tube data is an adiabatic, constant volume process with finite rate chemical kinetics. This model isolates the chemical kinetics from fluid dynamical considerations. The numerical problem consists of a set of ordinary differential equations for the temperature and the species

concentrations. The initial conditions are the pre-shock chemical concentrations and the post-shock thermodynamic conditions.

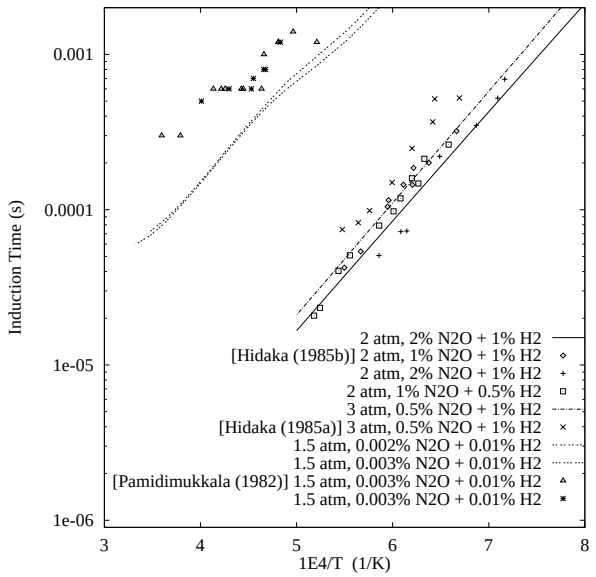

Figure 2: Comparison of H_2-N_2O-Ar reflected shock induction time data of Hidaka et al. (1985a), Hidaka et al. (1985b), and Pamidimukkala and Skinner (1982) with constant volume calculations using the mechanism of Frenklach et al. (1995).

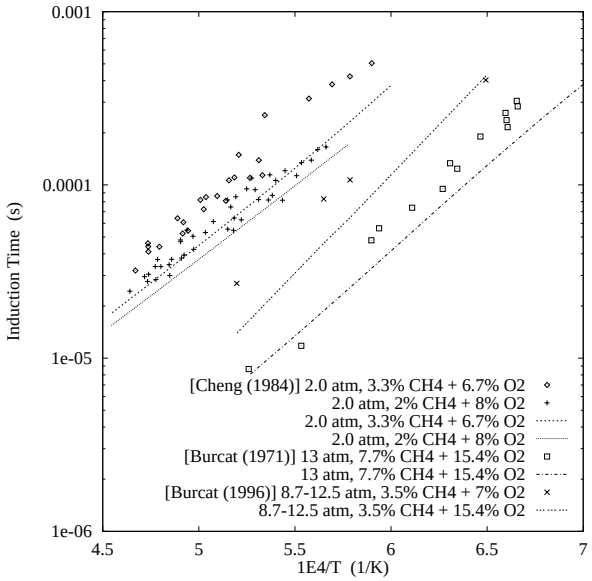

Figure 3: Comparison of CH_4-O_2-Ar reflected shock induction time data of Cheng and Oppenheim (1984), Burcat et al. (1971), and Burcat et al. (1996) with constant volume calculations using the mechanism of Frenklach et al. (1995).

Shock Tube Data (from the Literature)

Many experimental studies of reactions behind reflected shocks are available. In these experiments, the region near the shock tube end wall is monitored, usually by pressure transducers or spectroscopically, and one or more thermodynamic or species variables is measured over time. Induction time is variously defined by the delay after shock reflection before a sudden change in pressure, spectral emission or absorption, or other event. For cases where the induction zone is pronounced, most of these methods are comparable. For comparison with numerical results, we generally use the definition that the end of the induction zone is the point where the rate of increase of temperature is maximum. This is convenient because it does not involve arbitrary fractions, and it coincides with the point of maximum heat release.

The concept of induction time presupposes that the reactant mixture, subjected to an ignition source such as a shock wave or spark, will experience a rapid event consisting of changes in species concentrations, pressure, and temperature, following a period of relatively little activity. This supposition is reasonable for most cases because most combustion reactions involve a chain branching sequence. Under some conditions, for instance at very high or very low temperature, an induction time does not exist. At low temperature, it may be effectively infinite. At high temperature, the equilibrium state may not contain significant quantities of product, but rather may be largely dissociated. At some intermediate conditions, the induction time may be weakly defined, as the transition from reactants to products may be continuous and smooth.

An advantage of shock tube induction time data (over flame or flow reactor data) is that the post-shock conditions more closely resemble the conditions within a detonation. The thermodynamic condition within a fuel-air detonation varies (typically) from 1500 K and 40 atm (von Neumann state) to 3000 K and 20 atm (Chapman-Jouguet state). Many shock tube studies obtain these temperatures, but pressures above 5 atm are unusual. High Ar dilution is frequently used to increase induction times. Dilution with N_2 is unfortunately uncommon.

Validation Results

Several mechanisms (Frenklach et al. (1995), Baulch et al. (1994), Allen et al. (1995), Miller et al. (1983), and Miller and Bowman (1989)), each chosen for demonstrated performance with one or more mixtures of interest and for being fairly comprehensive, have been compared with a variety of experimental data. These comparisons were used to determine limits of validity (with respect to reactant concentrations, initial temperature, and initial pressure) for each mechanism. The mechanism of Frenklach et al. (1995) was found to be the most robust for the mixtures we have studied experimentally.

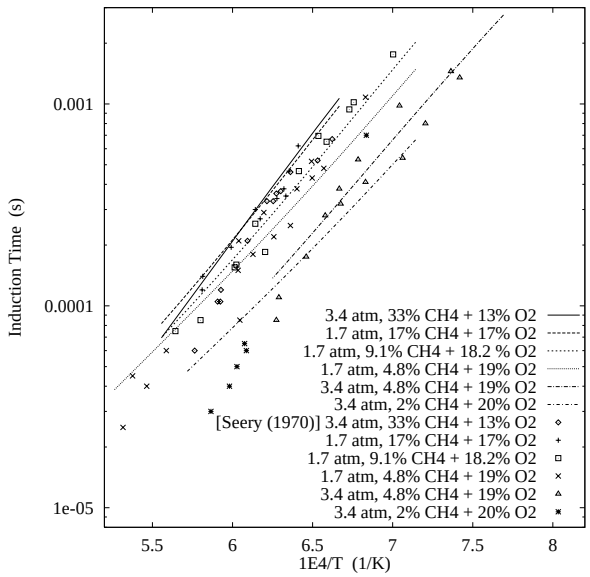

Figure 4: Comparison of CH_4-O_2-Ar reflected shock induction time data of Seery and Bowman (1970) with constant volume calculations using the mechanism of Frenklach et al. (1995).

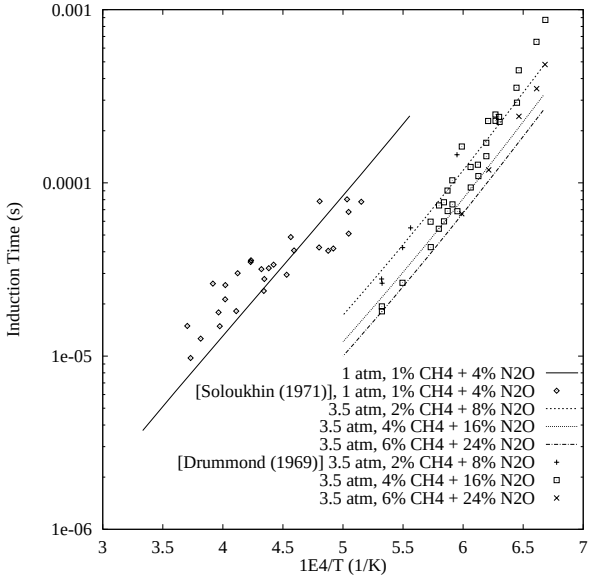

Figure 5: Comparison of CH_4-N_2O-Ar reflected shock induction time data of Soloukhin (1971) and Drummond (1969) with constant volume calculations using the mechanism of Frenklach et al. (1995).

Figs. 2-5 show comparisons for mixtures of H_2-N_2O-Ar, CH_4-O_2-Ar, and CH_4-N_2O-Ar. These comparisons show that calculations using the Frenklach et al. (1995) mechanism accurately match the shock tube data over a variety of conditions. Although the comparison conditions do not cover the full range of detonation conditions, the primary limitation is the Ar dilution, which can result in significantly different results from N_2 dilution. CH_4 reactions at air-like dilution with N_2 are difficult to validate because the induction times are very long, and the validity of the constant volume model is questionable.

ZND Reaction Zone Calculations

The ZND model of a detonation wave consists of a non-reactive, thin shock wave followed by an exothermic reaction zone (Zeldovich (1950)). The reaction zone is usually further decomposed into an induction zone, where heat release is small but radical species are created, and a thin region of rapid heat release where the reaction runs to completion. For CJ detonations, the shock strength is computed first with an equilibrium code (Stanjan). For computational purposes, the reaction zone solution is similar to the constant volume solution except the constraint on volume is replaced by the one-dimensional equations of fluid motion. The solution is marched forward in time and distance, and the reaction zone thickness is taken analogously to the constant volume induction time as the distance from the shock wave to the point of maximum heat release.

Cell Width Predictions

Cell width can not currently be computed or predicted directly. The ratio of cell width to reaction zone thickness (λ/Δ) is a function of other nondimensional parameters of the flow. For a system characterized by

a single reaction with activation energy E_a, energy release q, ratio of specific heats γ, and detonation Mach number M_{CJ}, we expect that

$$\frac{\lambda}{\Delta} = f(M_{CJ}, \gamma, \frac{q}{RT_0}, \frac{E_a}{RT_0})$$

While the general form of this function has not been found, certain useful approximations are possible. For instance, for a given fuel - oxidizer - diluent system at constant equivalence ratio and initial pressure, the function f is generally constant with respect to variation in dilution ratio. A slightly more general (but less rigorous) approach is illustrated in Figs. 6, 7, and 8. The cell width data from different test conditions are plotted together by using computed reaction zone thickness for each condition as the abscissa.

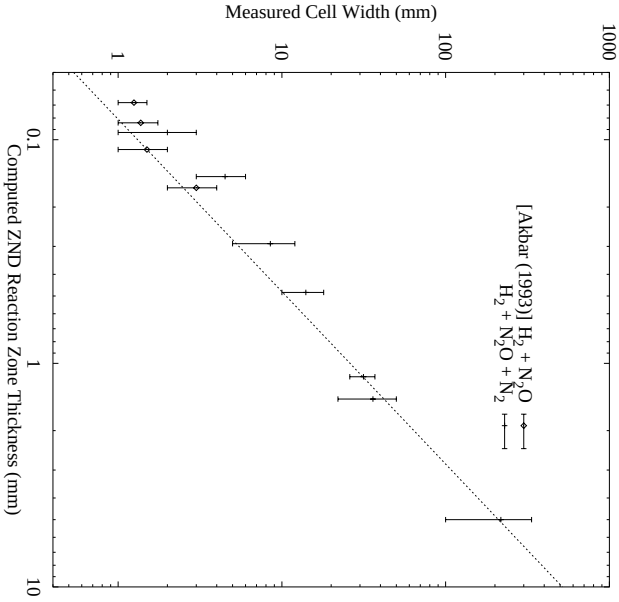

Figure 6: Correlation of cell width measurements from Akbar and Shepherd (1993) and the present study with computed ZND reaction zone thicknesses using the Frenklach et al. (1995) mechanism for stoichiometric H_2-N_2O mixtures in air and N_2

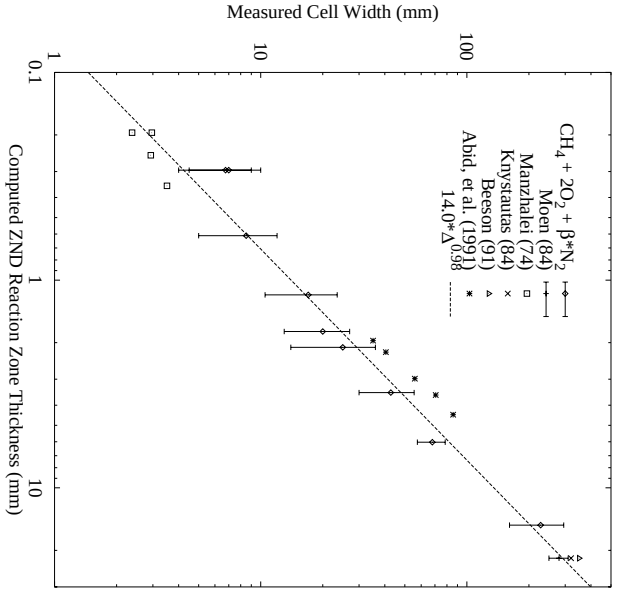

Figure 7: Correlation of cell width measurements from Moen et al. (1984), Manzhalei et al. (1974), Knystautas et al. (1984), Beeson et al. (1991), and the present study with computed ZND reaction zone thicknesses using the Frenklach et al. (1995) mechanism for stoichiometric CH_4-O_2 mixtures in N_2

For each fuel - oxidizer - diluent system, at constant equivalence ratio, cell width is found to obey a power law with respect to ZND reaction zone thickness. The experimental cell width data have been least-squares fit with power law curves, as shown in Figs. 6, 7, and 8. These power laws are given in Table 2, where the units of λ and Δ are mm.

Table 2: Cell Width - Reaction Zone Length Correlations

$$\begin{aligned} H_2 + N_2O + \beta N_2 &: \lambda = 26.06\Delta^{1.30} \\ H_2 + N_2O + \beta \text{air} &: \lambda = 40.83\Delta^{0.78} \\ CH_4 + 2O_2 + \beta N_2 &: \lambda = 14.45\Delta^{0.98} \\ CH_4 + 4N_2O + \beta N_2 &: \lambda = 9.73\Delta^{0.71} \end{aligned}$$

Note that while air is presented as a diluent along with N_2 in Fig. 8, it acts as an oxidizer also and thus H_2-N_2O-air constitutes an unique system. The undiluted H_2-N_2O data are considered to be a subset

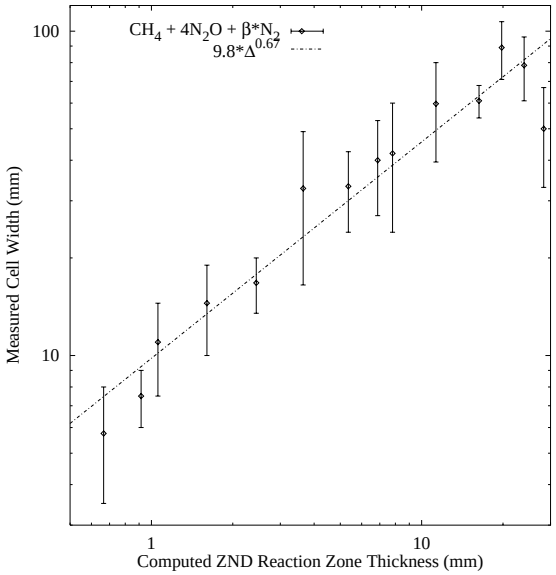

Figure 8: Correlation of cell width measurements with computed ZND reaction zone thicknesses using the Frenklach et al. (1995) mechanism for stoichiometric CH_4-N_2O mixtures in N_2

of the N_2 dilution data but not the air dilution data because O_2 is found to have a significant effect on N_2O mixtures even at very small concentrations.

Summary and Conclusions

Work reported here has followed two complementary approaches to characterizing the detonation parameters of certain mixtures of H_2-CH_4-N_2O-air. Experiments have been performed with mixtures of H_2-N_2O-O_2-N_2, CH_4-O_2-N_2, and CH_4-N_2O-O_2-N_2. Detonation velocities and cell widths have been measured and reported. Detonation velocities have been found to be very predictable by conventional thermochemical calculations. This experimental work is ongoing and the next study will involve mixtures containing NH_3.

Chemical kinetic models of the mixtures of interest have been compared to published experimental data and evaluated with respect to limits of validity. The mechanism of Frenklach et al. (1995) has been found to be valid for the mixtures mentioned above, although the validation studies have not explored the extremes of the relevant conditions. Correlations between chemical kinetic calculation results and detonation cell widths have been produced from the available cell width data. Extending, improving, and further validating the available reaction mechanisms is an active area of work. As new cell width data become available, the correlations will improve.

Acknowledgments

This work was performed for and supported by The Los Alamos National Laboratory.

References

Akbar, R. and J. Shepherd (1993, June). Detonations in N_2O-H_2-N_2-Air mixtures. Prepared for the Los Alamos National Laboratory Under Consultant Agreement C-4836.

Allen, M., R. Yetter, and F. Dryer (1995). The decomposition of nitrous oxide at $1.5 \leq P \leq 10.5$ atm and $1103 \leq T \leq 1173$ K. *Int. J. Chem. Kinet. 27*(9), 883–909.

Baulch, D., C. Cobos, R. Cox, P. Frank, G. Hayman, T. Just, J. Kerr, T. Murrells, M. Pilling, J. Troe, R. Walker, and J. Warnatz (1994). Evaluated kinetic data for combustion modeling: Supplement I. *J. Phys. Chem. Ref. Data 23*(6), 847–1033.

Beeson, H., R. McClenagan, C. Bishop, F. Benz, W. J. Pitz, C. Westbrook, and J. Lee (1991). Detonability of hydrocarbon fuels in air. In *Prog. Astronaut. Aeronaut.*, Volume 133, pp. 19–36.

Burcat, A., M. Dvinyaninov, and A. Lifshitz (1996). The effect of halocarbons on methane ignition. In *20th Symp. Int. Shock Waves.*

Burcat, A., K. Scheller, and A. Lifshitz (1971). Shock-tube investigation of comparative ignition delay times for C_1 - C_5 alkanes. *Combust. Flame 16*(1), 29–33.

Cheng, R. and A. Oppenheim (1984). Autoignition in methane-hydrogen mixtures. *Combust. Flame 58*(2), 125–139.

Drummond, L. (1969). Shock-induced reactions of methane with nitrous and nitric oxides. *Bull. Chem. Soc. Japan 42*, 285–289.

Frenklach, M., H. Wang, C. Bowman, R. Hanson, G. Smith, D. Golden, W. Gardiner, and V. Lissianski (1995). An optimized kinetics model for natural gas combustion. Technical report, Gas Research Institute. For more information, see HTTP://www.gri.org.

Hidaka, Y., H. Takuma, and M. Suga (1985a). Shock-tube studies of N_2O decomposition and N_2O-H_2 reaction. *Bull. Chem. Soc. Japan. 58*(10), 2911–2916.

Hidaka, Y., H. Takuma, and M. Suga (1985b). Shock-tube study of the rate constant for excited OH* ($^2\Sigma^+$) formation in the N_2O-H_2 reaction. *J. Phys. Chem. 89*(23), 4903–4905.

Kee, R., F. Rupley, and J. Miller (1989). Chemkin-II: A fortran chemical kinetics package for the analysis of gas-phase chemical kinetics. Technical Report SAND89-8009, Sandia National Laboratory.

Knystautas, R., C. Guirao, J. Lee, and A. Sulmistras (1984). Measurement of cell size in hydrocarbon-air mixtures and predictions of critical tube diameter, critical initiation energy, and detonability limits. In *Prog. Astronaut. Aeronaut.*, Volume 94, pp. 23–37.

Manzhalei, V., V. Mitrofanov, and V. Subbotin (1974). Measurement of inhomogeneities of a detonation front in gas mixtures at elevated pressures. *Combust. Explos. Shock Waves (USSR) 10*(1), 89–95.

Miller, J. and C. Bowman (1989). Mechanism and modeling of nitrogen chemistry in combustion. *Prog. Energy Combust. Sci. 15*, 287–338.

Miller, J., M. Smooke, R. Green, and R. Kee (1983). Kinetic modeling of the oxidation of ammonia in flames. *Combust. Sci. Technol. 34*, 149–176.

Moen, I., J. Funk, S. Ward, G. Rude, and P. Thibault (1984). Detonation length scales for fuel-air explosives. In *Prog. Astronaut. Aeronaut.*, Volume 94, pp. 55–79.

Pamidimukkala, K. and G. Skinner (1982). Resonance absorption measurements of atom concentrations in reacting gas mixtures. VIII. rate constants for $O+H_2=OH+H$ and $O+D_2=OD+D$ from measurements of O atoms in oxidation of H_2 and D_2 by N_2O. *J. Chem. Phys. 76*(1), 311–315.

Seery, D. and C. Bowman (1970). An experimental and analytical study of methane oxidation behind shock waves. *Combust. Flame 14*(1), 37–48.

Soloukhin, R. (1971). High-temperature oxidation of ammonia, carbon monoxide and methane by nitrous oxide in shock waves. In *13th Symp. Int. Combust. Proc.*, pp. 121–128.

Zeldovich, Y. (1950). On the theory of the propagation of detonation in gaseous systems. Technical Memorandum 1261, National Advisory Committee for Aeronautics. Translated from "K Teorri Rasprostranenia Detonantsii v Gasoobraznykh Sistremakh", Zhurnal Experimentalnoi i Teoreticheskoi Fiziki, T. 10, 1940.